Int. J. Electrochem. Sci., 15 **(2020)** 3003 – 3012, doi: 10.20964/2020.04.22

International Journal of
ELECTROCHEMICAL
SCIENCE
www.electrochemsci.org

Short Communication

Effect of Silicon Addition on Corrosion Behavior of Carbon Steel Rebar in Sulfuric Acid Environment

Hui Zhou, Yujie Wang[*], *Tengfei Ma*

Department of Architectural Engineering, North China Institute of Aerospace Engineering, Hebei, Langfang 065000, China
[*]E-mail: wangyj_80@foxmail.com

Received: 5 December 2019 / *Accepted:* 27 January 2020 / *Published:* 10 March 2020

Effects of silicon as an alloying element on corrosion resistance of carbon steel rebar in sulfuric acid environment were studied by a mass loss, polarization, open circuit potential and electrochemical impedance spectroscopy (EIS) analysis. The polarization results indicated that the corrosion potential was shifted to the more noble direction and the current density at the anode decreased slightly because of the Si addition. Based on EIS results, increasing the Si content revealed a significantly enhancement in the value of polarization resistance, indicating a high corrosion resistance of 0.9 wt% Si sample. The mass loss measurements exhibited a reduction of mass loss rate in carbon steel rebar with the increase of Si content which was in full accordance with the results of EIS analysis. The surface morphology of the carbon steel indicated a superlative more uneven and rough compared to the Si-containing steel reinforced concrete after 8 weeks exposure to the sulfuric acid environment.

Keywords: Alloyed carbon steel rebar; Silicon; Corrosion resistance; Electrochemical impedance spectroscopy; Reinforced concrete

1. INTRODUCTION

Carbon steel reinforced concrete is a material widely used in the construction industry worldwide because of its mechanical resistance and extraordinary structural strength [1, 2]. However, when this material is exposed to sea water or in a humid environment for long term, it is usually prone to severe corrosion attacks [3, 4]. Hence, corrosion degradation of the carbon steel rebar in aggressive media is currently considered as a major reason which leads to the reduction in the shelf lifetime of the reinforced concrete structures [5]. Many researchers have emphasized that because of the pore structure of the concrete, the diffusion and penetration of aggressive environment cannot be completely prevented [6-8]. Thus, improving corrosion resistance of steel rebar is a main factor to enhance the service life of reinforced concrete structures.

Numerous corrosion resistant rebar has previously been manufactured and used in the reinforced concrete at the aggressive environment, for example stainless steel rebar and epoxy-coated rebar [9-12]. However, due to the high cost of construction and production, these rebars are still used only in extremely aggressive environments [13]. Recent studies show that micro-alloyed steel rebar can be evaluated in the aggressive environment. By adding one or more anti-corrosion alloy elements, such as molybdenum, chromium, aluminum, nickel, copper and silicon (Si), the corrosion resistance of steel rebar can be improved in comparison with the general carbon steel rebar [14-17]. However, due to the low amount of alloying element used, the cost of production can be significantly reduced. Consequently, this alloyed rebar has great potential that can be used as a replacement for the carbon steel bars with a much longer service life in the aggressive environment [18]. Electrochemical impedance spectroscopy (EIS) method as a sensitive nondestructive instrument can be applied to consider the microstructure, physical, mechanical and electrical properties of the reinforced concrete [19, 20]. To describe the concrete-steel system, the EIS method has also made it possible to study the corrosion phenomenon of steel.

However, many studies have been done on alloy effects on corrosion behavior of steel reinforced concrete [21-23], study on the silicon content effect on the corrosion resistance of carbon steel are very limited. In this research, the effect of silicon addition on corrosion behavior of high-performance carbon steel rebar in sulfuric acid environment were investigated by EIS analysis.

2. MATERIALS AND METHOD

In this study, cylinder of ordinary Portland cement reinforced with carbon steel rebar with 6 mm diameter and 10 cm height were used to investigate the corrosion behavior of Si alloyed carbon steel rebar in acidic environment. Table 1 presents the chemical composition of the alloyed carbon steel rebars used in this study.

Table 1. Chemical composition of alloyed carbon steel rebar (wt%)

Alloys	C	Mn	Si	P	S	Cr	Fe
Carbon steel	0.4	0.001	0.00	0.001	0.003	0.001	Residual
0.2 wt% Si	0.4	0.01	0.19	0.004	0.003	0.01	Residual
0.5 wt% Si	0.4	0.01	0.48	0.004	0.003	0.01	Residual
0.9 wt% Si	0.4	0.01	0.91	0.004	0.003	0.01	Residual

Silicon carbide papers down to 2500# (LANHU, Germany) were employed to polish the samples. All samples were cleaned in acetone in an ultrasonic cleaner (Mophorn, China) and washed in distilled water. All electrochemical measurements were done in 1000 ml of a 10 wt% sulfuric acid (H_2SO_4) solution, which is believed to be the representative of the corrosive environment. In order to measure the gravimetric weight loss, the initial weights of the rebar were obtained using Metler prior to testing. The open circuit potential (OCP) for the various systems were periodically done using a high-impedance voltmeter with an input resistance of 10 MΩ. The homemade electrochemical cell was used to study the

electrochemical impedance spectroscopy (EIS) of the samples. In the three-electrode system, steel rebar samples were used as a working electrode and a saturated calomel electrode was applied as a reference electrode. The graphite was used as the counter electrode. EIS characterizations were performed in the frequency varied between 100 kHz and 0.1 mHz at the E_{OC} with AC perturbation ±10 mV. The polarization (CorrTest Instruments Corp., Ltd., China) measurement was conducted from 0.25V at 1 mV/s scanning rate. The morphologies of the samples were done by scanning electron microscope (SEM, FEI/Nova NanoSEM 450).

3. RESULTS AND DISCUSSION

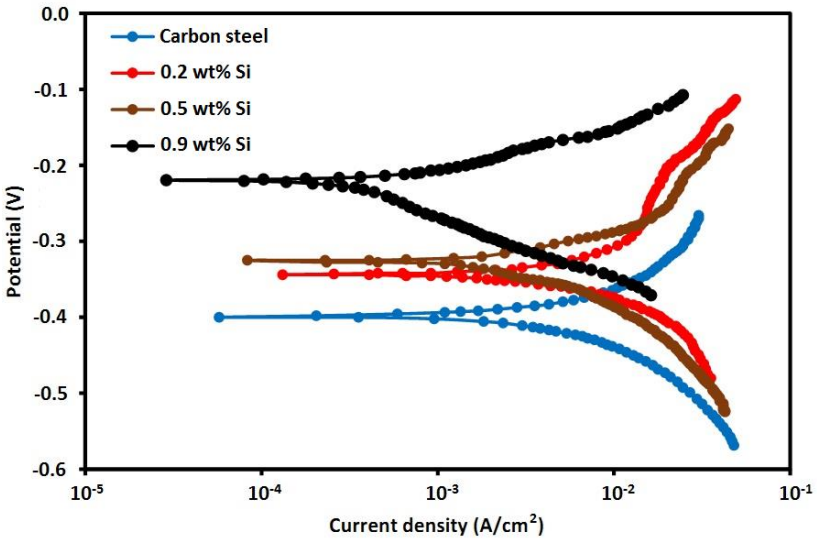

Figure 1. Polarization Plots of carbon steel rebar in the 10 wt% sulfuric acid solution at 25 °C temperature

The corrosion behavior of samples can be studied by the polarization curves. Thus, a polarization test was done to examine the electrochemical behavior of low alloy steel. Figure 1 indicates the polarization plots of the samples in 10 wt% H_2SO_4 solution at room temperature. Generally, all steel samples reveal no passivation and active corrosion behavior, showing the anodic current density enhanced constantly with the increasing applied potential. In this work, the corrosion potential were shifted to a more noble direction and the current density at the anode decreased slightly because of the Si addition, indicating the enhanced corrosion resistance with the addition of Si. The corrosion rates were determined by the Tafel extrapolation technique. According to Faraday's law, the corrosion rate can be measured by the corrosion current density [24]:

$$Corrosion\ rate\ \left(\frac{mm}{y}\right) = \frac{3.16\times10^{8} i_{corr} M}{z F_{\rho}} \qquad (1)$$

where M and i_{corr} are the molar mass of a metal and the corrosion current density, respectively. F and z are Faraday's constant and the number of electrons transferred for each metal atom, respectively. ρ is the metal density (g/cm^3).

Table 2. Fitting parameters of the samples attained from polarization plots in a 10 wt% H_2SO_4 solution at 25 °C.

Alloys	Corrosion current density (Acm^{-2})	Corrosion potential (V)	$-\beta_a$ ($mVdec^{-1}$)	β_c ($mVdec^{-1}$)	Corrosion rate (mm/year)
Carbon steel	0.00827	-0.395	22	52	7.6
0.2 wt% Si	0.00754	-0.346	25	59	5.2
0.5 wt% Si	0.00562	-0.328	28	56	4.3
0.9 wt% Si	0.00089	-0.218	33	54	2.1

The corrosion potential of the 0.9 wt% Si sample was significantly more positive than the other steels, which indicates that the self-corrosion potential increased after the addition of Si. Beyond that, the cathodic curves of samples shifted downwards when the Si content increased, which indicated that the cathode reaction rates were relatively lower at this stage [25]. The polarization data are summarized in table 2 which indicates the valuable effects of Si alloy. The differences in the corrosion rates might be due to the ohmic drop caused by the solution resistance, which occurred during the polarization test [26]. As shown in table 2, the reduction of corrosion rate with increasing Si content can be attributed to the the amount of Si in alloyed carbon steel rebar, which makes it more resistant towards corrosion and one of the most widely used carbon steel alloys in reinforced concretes. Furthermore, the resistance to pitting corrosion can be controlled by the use of Si. Moreover, the anodic Tafel slope (β_a), the cathodic Tafel slope (β_c) as well as the corrosion current density (i_{corr}) were determined from the Tafel extrapolation method. As shown in table 2, β_a and β_c values change with the concentration of Si. The change in Tafel slope values can be used to identify the inhibition mechanism (anodic or cathodic) for carbon steel, the concentration of the electrolyte, the composition of the working electrode and charge transfer coefficient [27]. The values of the cathodic Tafel slopes, significantly unchange with the Si addition, which implies that its influence on the cathodic reaction does not modify the mechanism of hydrogen evolution discharge [28]. Nevertheless, the values of the slopes of the anodic Tafel lines, change significantly with the addition of Si suggesting that there were blockage at the anodic reaction sites, and thereby affect the anodic reaction mechanism. Furthermore, with the increase of Si element, the anode Tafel slope increases which means Si element could promote the corrosion resistance of steel rebars in sulfuric acid solution.

In order to approve the polarization results and obtain a deeper insight into the influence of Si amount on the corrosion behavior of alloyed carbon steel, the EIS measurements were done in a 10 wt% sulfuric solution at 25 °C temperature.

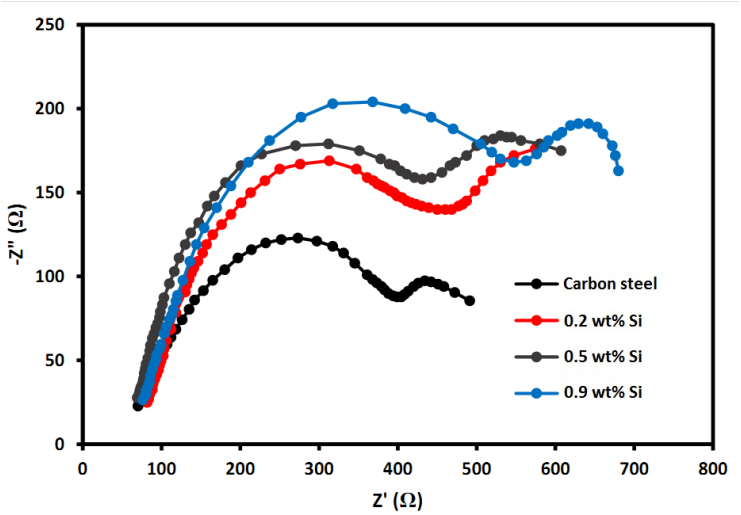

Figure 2. Nyquist plots of carbon steel rebar with different Si content in a 10 wt% sulfuric solution at 25 °C temperature

Figure 2 indicates Nyquist plots attained for the carbon steels with different Si contents under the open-circuit potential at a 10 wt% sulfuric solution. As revealed in Figure 2, two semicircles appeared in the electrochemical impedance spectra of the samples, indicating a capacitive semicircle and inductive loop in the high-medium and low frequency ranges, respectively. The capacitive semicircle characterizes the active state of the interface when the carbon steel is exposed to the sulfuric acid solution [29]. Furthermore, the inductive loop occurred at low frequency, can be associated to the adsorbed species onto the steel that develops the corrosion rate [30, 31].

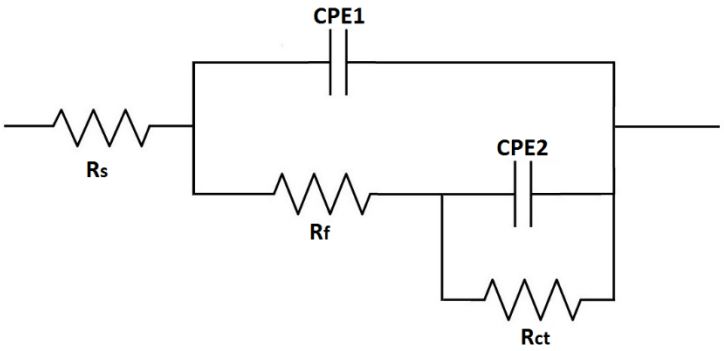

Figure 3. Equivalent impedance circuit for EIS data

Figure 3 shows an equivalent circuit model utilized to fit the above EIS results. R_s is the resistance of electrolyte solution. CPE1 and R_f are the capacitance and resistance of reinforced concrete, respectively. CPE2 and R_{ct} are the double-layer capacitance and the charge transfer resistance of the steel-electrolyte interface. Constant phase elements were often used for data fitting of depressed semicircles [32].

Table 3. Electrochemical parameters obtained from the fitting of the equivalent circuit model for different content of Si in a 10 wt% sulfuric solution at 25 °C temperature

Alloys	R_s (Ω cm^2)	R_f (Ω cm^2)	CPE_f (μF cm^{-2})	R_{ct} (Ω cm^2)	CPE_{dl} (μF cm^{-2})
Carbon steel	58.6	295	0.32	480	0.41
0.2 wt% Si	77.1	346	0.28	590	0.35
0.5 wt% Si	69.6	387	0.24	630	0.29
0.9 wt% Si	84.6	498	0.21	760	0.25

Table 4 shows the fitted EIS data. Polarization resistance, R_p ($R_p = R_f + R_{ct}$) is an assessable indicator to study the corrosion resistance of carbon steel in the corrosive environment. Thus, the higher the Rp value reveals a higher value of corrosion resistance for the sample [33]. Furthermore, the arc diameter in the Nyquist diagrams can be considered as R_p, and the reduction of the arc diameter reveals a decrease in R_p. Based on table 3, increasing the Si contents indicate a significantly enhancement in the value of R_p, indicating high corrosion resistance of 0.9 wt% Si samples.

Carbon steel samples with high Si content indicated relatively well corrosion resistance compared to carbon steel with low alloyed. The pitting corrosion appeared after a long-term exposure to aggressive environment, which can be related to high Si content.

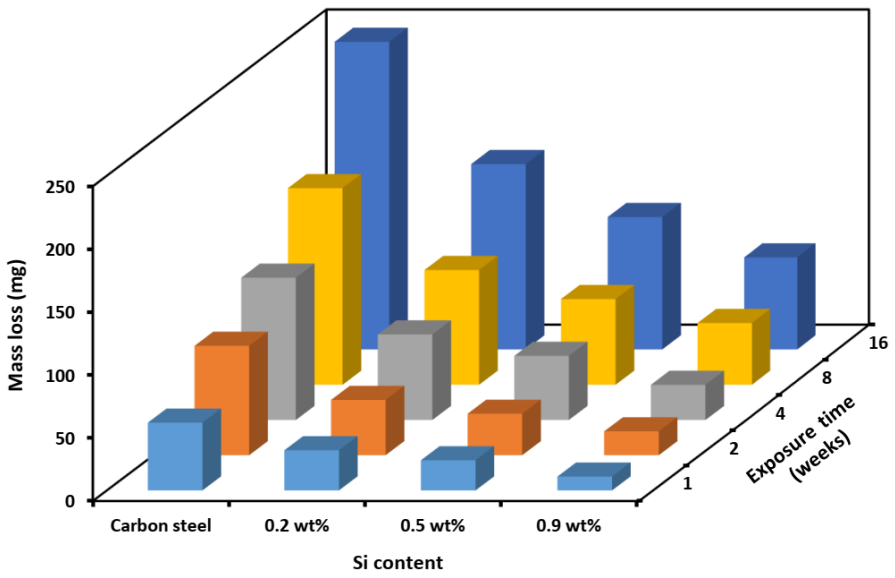

Figure 4. Mass loss of the samples with different Si content and various exposure times in a 10 wt% sulfuric solution at 25 °C temperature

After corrosion testing, the concrete samples were broken and the rebars were removed. Then the rebars were polished using sandpaper and steel brushes to eliminate residual rust and concrete from the surface of steels. Then, they were soaked for 15 min in a 10% sulfuric acid, and re-polished. Finally, they were placed in the oven to slowly dry, and weighed with 0.01 g accuracy. As shown in Fig. 4, with increasing exposure time, the mass loss of the steel rebars in 10 wt% sulfuric acid solution were

increased. Furthermore, As the Si content increases, the mass loss becomes lower and lower, indicating reduction of mass loss rate in carbon steel with the increase of Si content. According to the researches by Melchers [34] and Tamura [35], the decreased mass-loss rate of the rebar can be attributed to the mechanical isolation effect of the rust layer on the direct contact between the rebar matrix and the electrolyte solution. This is in full accordance with the results of EIS analysis.

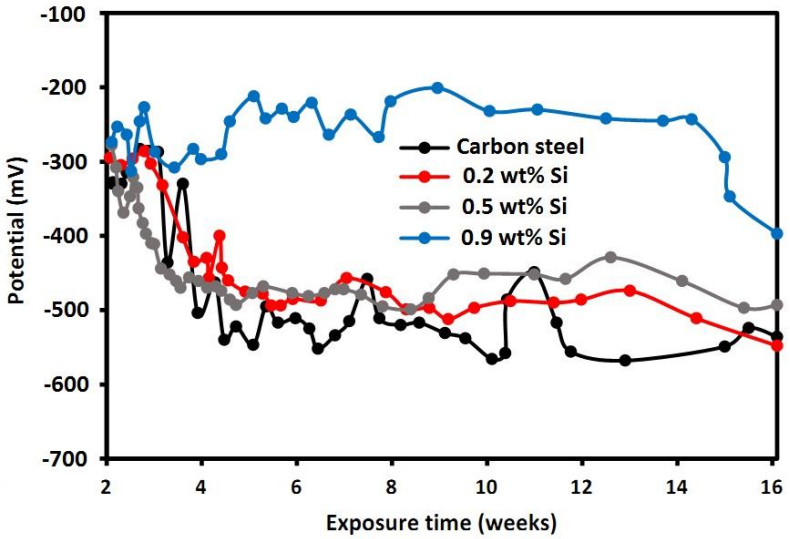

Figure 5. Open circuit potential of the samples with different Si content and various exposure time in a 10 wt% sulfuric solution at 25 °C temperature

Half-cell potential measurement technique is a well-known methods to determine the corrosion of rebar in concrete [36]. In this technique, the potential difference between a reference electrode and rebar embedded into concrete is measured in according to ASTM C-876 [37]. Figure 5 reveals the potential measurement for 16 weeks. As shown, with the increase the Si content in carbon steel rebar, the potential of samples shift towards more positive values which is noticeable in the rebar with 0.9 wt% Si content.

The chemical and electrochemical measurements support only the final conclusions about the effectiveness of adding Si to the corrosion resistance of carbon steels. Thus, surface morphology analysis was done to consider the corrosion behavior of Si-containing carbon steel rebars. Figure 6 indicates SEM images of the samples with different Si content after 8 weeks exposure in 10 wt% H_2SO_4 solution. No pitting appeared on the sample with 0.9 wt% Si. The surface of the carbon steel was uneven and rough compared to the Si-containing carbon steels. Therefore, corrosion damage to the carbon steels reduced with increasing Si content, indicating that the Si addition delays the corrosion process.

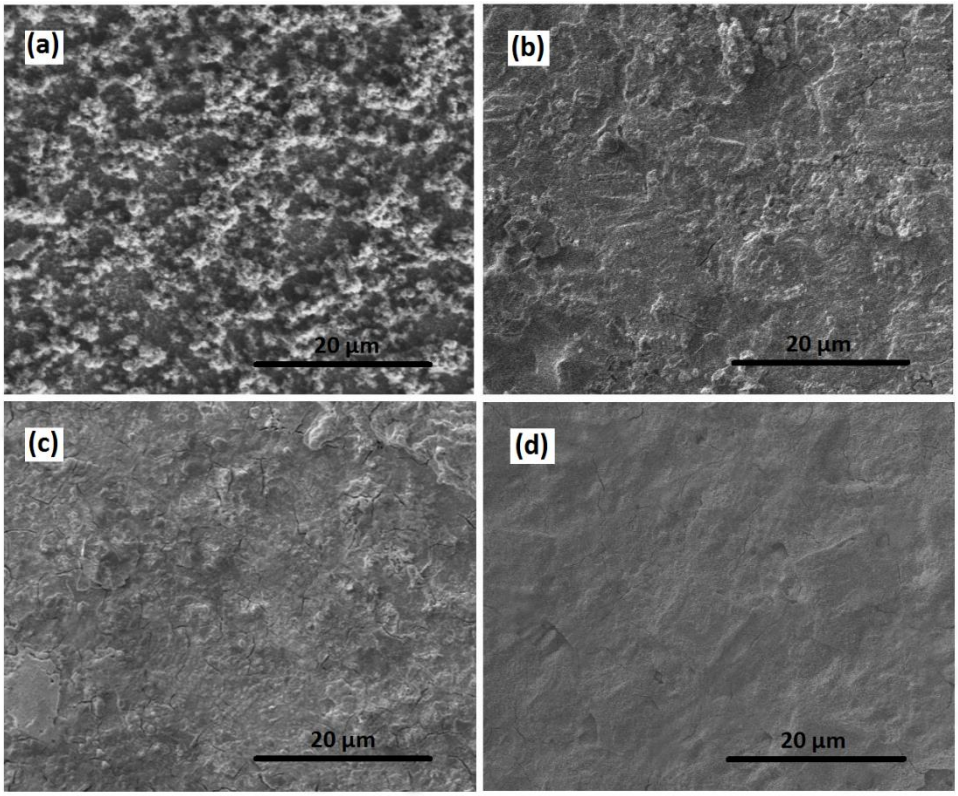

Figure 6. SEM images of the samples with different Si content (a) carbon steel (b) 0.2 wt% (c) 0.5 wt% (d) 0.9 wt% after 8 weeks exposure time in a 10 wt% sulfuric solution at 25 °C temperature

4. CONCLUSIONS

Recent studies show that the micro-alloyed steel rebars can improve the corrosion behavior of steel reinforced concretes in an aggressive environment. Here, silicon as an alloying element was selected to study the alloy effects on corrosion resistance of carbon steel rebar in sulfuric acid environment. Mass loss, polarization, OCP and EIS analysis were used to investigate corrosion behavior of micro-alloyed steel rebar. The polarization results indicate that the corrosion potential had shifted to a more noble direction and the current density at the anode decreased slightly because of the Si addition. Based on EIS results, increasing the Si contents indicate a significantly enhancement in the value of polarization resistance, indicating a high corrosion resistance of 0.9 wt% Si samples. The mass loss measurements showed a decrease when the Si content increased, indicating a reduction of mass loss rate in carbon steel with the increase of Si content which was in full accordance with the results of EIS analysis. The OCP results show that by increasing the Si content in a carbon steel rebar, the corrosion potential of the samples had shifted towards more positive values which was noticeable in the rebar with 0.9 wt% Si content. The surface morphology of the carbon steel indicated superlative more uneven and rough compared to the Si-containing carbon steels after 8 weeks exposure to 10 wt% sulfuric acid environments.

ACKNOWLEDGEMENTS
This study was supported by Frame Structure with Special-shaped Columns in High Intensity Zone Analysis and Application of Seismic Performance, Construction of Science and Technology Guiding Projects in Hebei Province China (Grant No. 2008-201).

References

1. W. Li, S.C.M. Ho and G. Song, *Smart Materials and Structures*, 25 (2016) 045017.
2. X. Feng, J. Liu, C. Hang, Z. Lu, Y. Jiang, Y. Xu and D. Chen, *International Journal of Electrochemical Science*, 11 (2016) 5226.
3. J. Xiao, C. Qiang, A. Nanni and K. Zhang, *Construction and Building Materials*, 155 (2017) 1101.
4. J. Hu, G. Shaokang, C. Zhang, C. Ren, C. Wen, Z. Zeng and L. Peng, *Surface and Coatings Technology*, 203 (2009) 2017.
5. J.O. Okeniyi, O.A. Omotosho, C.A. Loto and A.P.I. Popoola, *Asian Journal of Scientific Research*, 8 (2015) 454.
6. X. Chen, L. Xu and S. Wu, *Journal of Materials in Civil Engineering*, 28 (2015) 04015110.
7. H. Shan, Z. Wang, J. Xu and L. Jiang, *International Journal of Electrochemical Science*, 13 (2018) 1120.
8. J. Hu, C. Zhang, S. Guan, L. Wang, S. Zhu, S. Chen, J. Gao, E. Meng, S. Hou and B. Cui, *Materials Letters*, 64 (2010) 2569.
9. Y. Zhang, *International Journal of Electrochemical Science*, 14 (2019) 9347.
10. B. Shang, Y. Ma, M. Meng and Y. Li, *Materials and Corrosion*, 70 (2019) 1657.
11. Y. Zhang, K. Bai, Z. Fu, C. Zhang, H. Zhou, L. Wang, S. Zhu, S. Guan, D. Li and J. Hu, *Applied Surface Science*, 258 (2012) 2939.
12. K. Bai, Y. Zhang, Z. Fu, C. Zhang, X. Cui, E. Meng, S. Guan and J. Hu, *Materials Letters*, 73 (2012) 59.
13. J. Hu, C. Zhang, B. Cui, K. Bai, S. Guan, L. Wang and S. Zhu, *Applied Surface Science*, 257 (2011) 8772.
14. G. Xing and O.E. Ozbulut, *Engineering Structures*, 126 (2016) 53.
15. A. Cladera, E. Oller and C. Ribas, *Journal of Materials in Civil Engineering*, 26 (2013) 04014084.
16. G. Cao, L. Wang, Z. Fu, J. Hu, S. Guan, C. Zhang, L. Wang and S. Zhu, *Applied Surface Science*, 308 (2014) 38.
17. C. Li, S. Hu, L. Yang, J. Fan, Z. Yao, Y. Zhang, G. Shao and J. Hu, *Chemistry–An Asian Journal*, 10 (2015) 2733.
18. M. Serdar, L.V. Žulj and D. Bjegović, *Corrosion science*, 69 (2013) 149.
19. S. Kakooei, H.M. Akil, A. Dolati and J. Rouhi, *Construction and Building Materials*, 35 (2012) 564.
20. P. Shao, L. Ding, J. Luo, Y. Luo, D. You, Q. Zhang and X. Luo, *ACS applied materials & interfaces*, 11 (2019) 29736.
21. M. Liu, X. Cheng, X. Li, Z. Jin and H. Liu, *Construction and Building Materials*, 93 (2015) 884.
22. Q. Zeng, J. Sun, W. Emori and S. Jiang, *Journal of Materials Engineering and Performance*, 25 (2016) 1773.
23. D. Song, J. Hao, F. Yang, H. Chen, N. Liang, Y. Wu, J. Zhang, H. Ma, E.E. Klu and B. Gao, *Journal of Alloys and Compounds*, 809 (2019)
24. A.D. King, N. Birbilis and J.R. Scully, *Electrochimica Acta*, 121 (2014) 394.

25. L. Yang, G. Yi, Y. Hou, H. Cheng, X. Luo, S.G. Pavlostathis, S. Luo and A. Wang, *Biosensors and Bioelectronics*, 141 (2019) 111444.
26. N. Naderi, M. Hashim and J. Rouhi, *International Journal of Electrochemical Science*, 7 (2012) 8481.
27. Y. Zhou, S. Xu, L. Guo, S. Zhang, H. Lu, Y. Gong and F. Gao, *RSC Advances*, 5 (2015) 14804.
28. A. Ansari, M. Znini, I. Hamdani, L. Majidi, A. Bouyanzer and B. Hammouti, *Journal of Materials and Environmental Science*, 5 (2014) 81.
29. F. Husairi, J. Rouhi, K. Eswar, A. Zainurul, M. Rusop and S. Abdullah, *Applied Physics A*, 116 (2014) 2119.
30. N. Odewunmi, S. Umoren and Z. Gasem, *Journal of Industrial and Engineering Chemistry*, 21 (2015) 239.
31. P. Shao, X. Duan, J. Xu, J. Tian, W. Shi, S. Gao, M. Xu, F. Cui and S. Wang, *Journal of hazardous materials*, 322 (2017) 532.
32. M.Y.K. Meynaq, K. Shimizu, M.S. Aghbolagh, S. Tesfalidet and B. Lindholm-Sethson, *Journal of colloid and interface science*, 482 (2016) 212.
33. J. Rouhi, S. Mahmud, S.D. Hutagalung and S. Kakooei, *Journal of Micro/Nanolithography, MEMS, and MOEMS*, 10 (2011) 043002.
34. R.E. Melchers, *Corrosion science*, 68 (2013) 186.
35. H. Tamura, *Corrosion science*, 50 (2008) 1872.
36. F. Husairi, J. Rouhi, K. Eswar, C.R. Ooi, M. Rusop and S. Abdullah, *Sensors and Actuators A: Physical*, 236 (2015) 11.
37. B. Assouli, G. Ballivy and P. Rivard, *Corrosion Engineering, Science and Technology*, 43 (2008) 93.